Temperature and Magnetic Field Effects on the Luminescence of $Tl_2Pt(CN)_4$

B. Weissbart, A. L. Balch,* and D. S. Tinti*

Department of Chemistry, University of California, Davis, California 95616

Received July 17, 1992

The luminescence spectra and decay kinetics of $Tl_2Pt(CN)_4$ are studied as a function of temperature at ≤30 K and of applied magnetic field at 1.4 K. Two major emission bands are seen which peak at ≈455 and ≈575 nm. Their relative intensities depend strongly on the excitation wavelength and temperature. The 455-nm band has an excitation maximum at ≈375 nm while that of the 575-nm band occurs at ≈335 nm. For either of these excitation wavelengths, the relative intensity of the 455-nm band is a minimum and that of the 575-nm band is a maximum at ≈17 K. The lifetimes at 1.4 K are 77 and 62 μs for the 455- and 575-nm bands, respectively. These are shortened by Zeeman fields with the magnitude of the effect proportional to the square of the field strength and dependent on the orientation of the field relative to the crystal axes of $Tl_2Pt(CN)_4$. The lifetimes also show abrupt decreases at ≈12 and ≈5 K for the 455- and 575 nm-bands, respectively. The intensity and kinetic data are interpreted in terms of a model which involves emissive triplet states for both bands.

Introduction

The spectroscopic properties of compounds of tetracyanoplatinate, $Pt(CN)_4^{2-}$, have been widely studied in a variety of salts with alkali and alkaline earth metal cations[1] and in fluid solution.[2] The crystals are typically colored and are characterized by pseudo-one-dimensional columnar chains of the planar anions. Significant interaction occurs along the chain between adjacent anions. This causes the spectroscopic properties of the salts to depend strongly on the Pt–Pt distance. Two major luminescence bands are seen, which have been assigned nominally as fluorescence from a free exciton state and phosphorescence from a state localized on the $Pt(CN)_4^{2-}$ anion (self-trapped exciton), respectively.[1] Aqueous solutions of $Pt(CN)_4^{2-}$ at room temperature are also emissive. However, the emissions in solution are due to oligomers of $Pt(CN)_4^{2-}$, arising from the same sort of stacking interactions that occur in the crystals; no emission from simple monomers of $Pt(CN)_4^{2-}$ has been established.[2]

Although various possibilities have been proposed for the orbital energies of the monomer,[1-5] the consensus appears to be that the lowest energy excitation in the columnar solids and solution oligomers derives from the $\pi^*(Pt\text{–}6p_z + CN\text{-}\pi^*, a_{2u}) \leftarrow d(Pt\text{-}5d_{z^2}, a_{1g})$ excitation in the D_{4h} point group of $Pt(CN)_4^{2-}$. In a molecular orbital scheme, this arises since the Pt $5d_{z^2}$ and $6p_z$ orbitals of the monomers each overlap in the stack direction to form bands or groups of orbitals that are roughly symmetrically displaced, whereas the remaining orbitals of the monomer interact less strongly. Since the nodal properties of the orbitals at the top of the d_{z^2} band are Pt–Pt antibonding, while those at the bottom of the p_z band are bonding, the lowest energy excitation becomes $p\sigma \leftarrow d\sigma^*$. The $^{1,3}A_{2u}$ states of the monomer that obtain from $p_z \leftarrow d_{z^2}$ are thus stabilized due to the stacking interactions, proportional to the inverse cube of the Pt–Pt distance.[1]

A noncolumnar, crystalline form of $Pt(CN)_4^{2-}$ has also been reported that involves covalent Pt–Tl bonds (3.14 Å) and discrete $Tl_2Pt(CN)_4$ octahedral molecules at C_i sites.[6] These crystals are colorless but are also intensely luminescent. Qualitative considerations suggested that the lowest energy excitation of $Tl_2Pt(CN)_4$ in the D_{4h} point group is $\pi^*(Tl\text{-}6p_z, a_{2u}) \leftarrow d(Pt\text{-}5d_{z^2}, a_{1g})$. The intermolecular Pt–Pt distances are all greater than 6 Å, and the normals to the anion planes make large angles with the Pt–Pt directions. Hence, stacking interactions between the anions are absent. However, the filled 6s and empty $6p_z$ orbitals of the axial Tl(I) in $Tl_2Pt(CN)_4$ can act similarly to the Pt(II) $5d_{z^2}$ and $6p_z$ orbitals, respectively, in the columnar systems to stabilize the resulting $^{1,3}A_{2u}$ states. The luminescence was assigned on the basis of its moderately long lifetime at 300 K (0.25 μs) as originating from this $^3A_{2u}$ excited state.[6] Recent studies have shown that the lifetime lengthens considerably at lower temperatures (77.5 μs at 4.2 K), which was attributed to emission from the Boltzmann equilibrated, spin–orbit components of the $^3A_{2u}$ state.[7] Relativistic extended Hückel calculations support a $^3A_{2u}$ assignment for the lowest excited state,[8] but relativistic density functional calculations indicate that the HOMO is mainly Pt-$5d_{xy}$ (b_{2g}), not Pt-$5d_{z^2}$, predicting a $^3B_{1u}$ assignment for the emissive state.[5] An apparently different form of $Tl_2Pt(CN)_4$, a pale yellow powder, has also been reported from a different synthetic procedure.[9]

We report herein the results of additional, extended studies of the luminescence of $Tl_2Pt(CN)_4$ at low temperatures for the two reported forms of the material. Both forms show two major emission bands with similar characteristics. The spectra and decay kinetics of the bands have been investigated as a function of temperature and applied magnetic field strength, focusing on the colorless crystals. The results support a nominal triplet assignment for the excited state of both of the major emission bands.

(1) Gliemann, G.; Yersin, H. *Struct. Bonding* **1985**, *62*, 87 and references therein.
(2) Schinder, J. W.; Fukada, R. C.; Adamson, A. W. *J. Am. Chem. Soc.* **1982**, *104*, 3596. Lechner, A.; Gliemann, G. *J. Am. Chem. Soc.* **1989**, *111*, 7469.
(3) Thomas, T. W.; Underhill, A. E. *Chem. Soc. Rev.* **1972**, *1*, 99. Interrante, L. V., Ed. *Extended Interactions between Metal Ions*; American Chemical Society: Washington, DC, 1974. Keller, H. J., Ed. *Low-Dimensional Cooperative Phenomena*; Plenum Press: New York, 1975. Keller, H. J., Ed. *Chemistry and Physics of One-Dimensional Metals*; Plenum Press: New York, 1977. Miller, J. S., Ed. *Extended Linear Chain Compounds*; Plenum *Press*: New York, 1982.
(4) Interrante, L. V.; Messmer, R. P. *Chem. Phys. Lett.* **1974**, *26*, 225. Isci, H.; Mason, W. R. *Inorg. Chem.* **1975**, *14*, 905. Marsh, D. G.; Miller, J. S. *Inorg. Chem.* **1976**, *15*, 720. Miller, J. S.; Marsh, D. G. *Inorg. Chem.* **1976**, *15*, 2293. Cowman, C. D.; Gray, H. B. *Inorg. Chem.* **1976**, *15*, 2823. Lopez, J. P.; Yang, C. Y.; Case, C. A. *Chem. Phys. Lett.* **1982**, *91*, 353.
(5) Ziegler, T.; Nagle, J. K.; Snijders, J. G.; Baerends, E. J. *J. Am. Chem. Soc.* **1989**, *111*, 5631.
(6) Nagle, J. K.; Balch, A. L.; Olmstead, M. M. *J. Am. Chem. Soc.* **1988**, *110*, 319.
(7) (a) Nagle, J. K.; Lacasce, J. H.; Dolan, P. J.; Corson, M. R.; Assefa, Z.; Patterson, H. H. *Mol. Cryst. Liq. Cryst.* **1990**, *181*, 359. (b) Nagle, J. K. Private communication.
(8) Assefa, A.; DeStefano, F.; Garepapaghi, M. A.; LaCasce, J. H.; Ouellete, S.; Corson, M. R.; Nagle, J. K.; Patterson, H. H. *Inorg. Chem.* **1991**, *30*, 2868.
(9) Truitt, L. E.; Freeman, W. A.; Williams, J. M. *Inorg. Synth.* **1982**, *21*, 153.

0020-1669/93/1332-2096$04.00/0

Experimental Section

Samples of $Tl_2Pt(CN)_4$ were prepared by following the two reported schemes using reagent grade materials. The colorless, monoclinic crystals were grown by slow diffusion between aqueous solutions of $K_2Pt(CN)_4$ and $TlNO_3$ or $TlCH_3CO_2$, as described previously by Nagle et al.[6] The crystals formed mainly as *bc* plates that were elongated along the *b* axis with maximum dimensions of ca. $2 \times 0.5 \times 0.05$ mm^3 for good-quality crystals. Pale yellow powders of $Tl_2Pt(CN)_4$ were obtained, as described by Truitt et al.,[9] by mixing aqueous solutions of $BaPt(CN)_4$ and Tl_2SO_4, removing the $BaSO_4$ precipitate by filtration, and cooling the filtrate to precipitate the desired material. Samples from the two preparations were used without further purification.

A comparison of the lattice parameters of the orthorhombic, pale yellow form[9] with those of the monoclinic, colorless crystals[6] implies a gross difference between the two solids. However, this is not necessarily the case. The twelve *d* spacings given by Truitt et al.[9] for the powder pattern of the colored form ($0 \le 2\theta \le 40°$) can be indexed equally well (similar sums for the squared deviations) to yield either their orthorhombic cell or the monoclinic cell of Nagel et al.[6] The calculated densities of the two forms, based on four and two molecules per unit cell, respectively, are also identical (5.44 g/cm^3). To check this further, powder patterns were obtained for samples prepared by the two schemes, and the results were compared with the powder pattern calculated from the crystal structure parameters of the colorless crystals. The *d* spacings and intensities of the observed powder patterns ($0 \le 2\theta \le 75°$) are in fact very similar for the two forms and agree with the calculated pattern. This strongly suggests that the reported lattice parameters for the pale yellow powder are incorrect. It appears that in the previous work the refinement may have been restricted to orthorhombic or greater symmetry. On the basis of the powder pattern data, we conclude that the pale yellow powder and colorless crystal forms of $Tl_2Pt(CN)_4$ are essentially identical and that the yellow color in the one form arises from impurities.

Conventional emission spectra were excited with a 75-W Xe, 100-W Hg, or 450-W Xe lamp, in conjunction with a 0.25-m monochromator and/or filters, and recorded with a 1.0-m Czerny–Turner spectrometer equipped with an RCA C31034 photomultiplier tube. Excitation spectra were detected with the 1-m spectrometer by scanning the 0.25-m monochromator with 3-nm slits and a Xe lamp as the excitation source. Pulsed excitation for time-resolved spectra and decay measurements employed a N_2 laser (337.1 nm, pulse width $\le$10 ns) with the spectrometer output processed by a box-car and signal averager (minimum dwell time 200 ns), respectively. All reported spectra are uncorrected for instrumental sensitivity or lamp output. For variable temperatures between 4.2 and 77 K, the sample was in intimate contact with a metal block whose temperature was determined using a calibrated carbon resistor.

A superconducting, split-coil magnet provided static magnetic fields of $\le$3.2 T. The spectra and decays in the Zeeman field were obtained with the orientation of the magnetic field perpendicular to the propagation directions of the exciting and emitted light.

Results

Optical Spectra. Figure 1 compares the emission spectrum of colorless crystals of $Tl_2Pt(CN)_4$ at 300, 77, and 1.4 K. In agreement with the original report,[6] only a single maximum at 448 (±2) nm with a fwhm of ≈2800 cm^{-1} occurs at 300 K. Its measured polarization ratio in (100) is $I_b/I_c = 0.8$ at 300 K. This band progressively red-shifts and narrows with decreasing temperature. At 1.4 K, the maximum occurs at 457 (±1) nm with a fwhm of ≈1500 cm^{-1}. At $\le$77 K, a second emission band clearly resolves. Its maximum occurs at 577 (±3) nm with a fwhm of ≈2600 cm^{-1} at 1.4 K. Both bands appear similarly and uniformly polarized in (100) with $I_b/I_c = 0.6$ at 1.4 K. Neither band shows vibronic structure under any of the excitation or detection conditions employed. In the following, we refer to the ≈455- and ≈575-nm bands as the blue and red bands, respectively. Their properties are summarized in Table I.

Uncorrected excitation spectra of the colorless crystals are included in Figure 1. When the blue emission band is monitored, a single photoexcitation band is seen which narrows with decreasing temperature. At 1.4 K, the band peaks at 375 (±2) nm with a fwhm of ≈3000 cm^{-1} and shows no overlap with the blue emission band. The observed peak wavelength agrees with

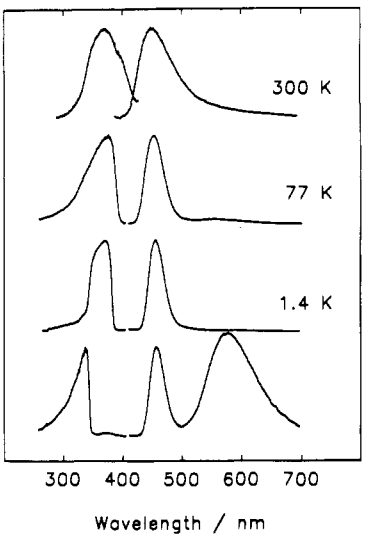

Figure 1. Conventional emission and photoexcitation spectra (uncorrected) of $Tl_2Pt(CN)_4$ at 300, 77, and 1.4 K. At 300 and 77 K, the emission spectra were excited at 370 nm and the photoexcitation spectra monitored at 455 nm. At 1.4 K, spectra are shown for (top) excitation at 370 nm and detection at 455 nm and (bottom) excitation at 330 nm and detection at 575 nm. The shoulder in the photoexcitation spectrum at 300 K is associated with the excitation source.

Table I. Properties of the Emission Bands of $Tl_2Pt(CN)_4$

temp/K	emiss max/nm	fwhm/ cm^{-1}	lifetime/ μs	emiss max/nm	fwhm/ cm^{-1}	lifetime/ μs
300	448	2800	0.25[a]			
77	453	1700	1.4	565	3000	
1.4	457	1500	77	577	2600	62

[a] Reference 6.

the single maximum at 370 nm seen in the room-temperature absorption spectrum of a mulled sample. The absorption of a ≈0.05 mm thick *bc* plate at 1.4 K shows only a steep onset beginning at ≈395 nm, which we suppose corresponds to the onset of the 375-nm photoexcitation maximum and the room-temperature 370-nm absorption maximum. The red band shows a principal photoexcitation maximum at 1.4 K of 335 (±2) nm. This is evident only as an unresolved shoulder at 77 K. Excitation at 370 or 330 nm leads to similar emission spectra at 300 and 77 K, which consist predominantly of the blue band. However, as shown in Figure 1, the two excitation wavelengths yield very different relative intensities for the blue and red bands at 1.4 K.

For excitation at either 370 or 330 nm, the relative intensity of the red band is a maximum between 1.4 and 77 K. Example spectra at intermediate temperatures are shown in Figure 2 for 370-nm excitation. Figure 3 gives the relative peak intensities of the blue, I_{blue}, and red, I_{red}, bands as a function of temperature for 370- (top) and 330-nm (bottom) excitation, normalized to unit I_{blue} for $T \le 8$ K. For both excitations, I_{red} has its maximum and I_{blue} has its minimum at ≈17 K. An Arrhenius plot of the peak intensity ratio, I_{red}/I_{blue}, is shown in Figure 4. At low temperatures (≈5–15 K) for 370-nm excitation, the ratio appears thermally activated with an energy of ≈100 cm^{-1}. At higher temperatures (≈20–40 K) for both excitations, the ratio appears thermally deactivated with an energy of ≈65 cm^{-1}. As shown in Figure 5, the peak wavelength of the blue band also changes abruptly in the temperature range 10–20 K by 2.9 ± 0.1 nm (140 ± 5 cm^{-1}). No corresponding sudden wavelength shift could be detected for the red band. Its peak wavelength decreases monotonically with increasing temperature between 1.4 and 77 K.

The differences in excitation spectra suggest that the blue and red emission bands may not arise from a common center. On the basis of the disagreement between the photoexcitation and

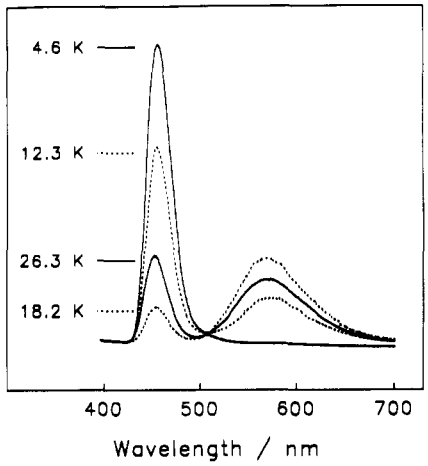

Figure 2. Conventional emission spectra of $Tl_2Pt(CN)_4$ between 4 and 27 K, showing the intensity changes that occur in the blue and red emission bands for excitation at 370 nm.

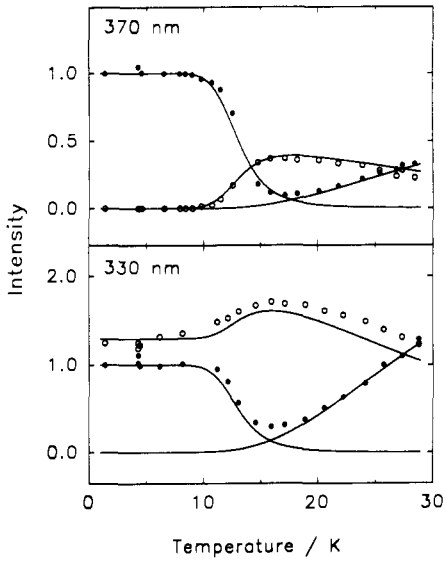

Figure 3. Relative peak intensities of the blue (filled circles) and red (open circles) emission bands of $Tl_2Pt(CN)_4$ for 370- (top) and 330-nm (bottom) excitation as a function of temperature. The solid lines are the relative intensities calculated from the kinetic model discussed in the text.

absorption maxima, the red emission band may be due to an adventitious impurity or defect incorporated into the crystals of $Tl_2Pt(CN)_4$ during preparation. However, we have not detected any significant differences in the relative intensities of the blue and red bands under the same experimental conditions among different samples. These include microcrystalline and single-crystal samples, samples from different preparation batches, and samples prepared under different preparation conditions. In particular, samples obtained from TlX ($X = NO_3^-$, $CH_3CO_2^-$) and $K_2Pt(CN)_4$ in 2:1, 5:1, and 1:5 molar ratios produced similar spectra.[10] Hence, we cannot discount either atypical relaxation among the excited states of a single center or two intrinsic centers as possible explanations for the observed spectra.

The impure, pale yellow form of $Tl_2Pt(CN)_4$ is also emissive. However, not unexpectedly, its spectra are considerably more complicated than those of the colorless crystals. It shows the

(10) This argues against assigning either of the bands to $KTlPt(CN)_4$ or $K_2Pt(CN)_4$, which might be incorporated into the crystals of $Tl_2Pt(CN)_4$ during their growth. Further, the starting materials at 77 K do not emit at the wavelengths of the observed bands for excitation at 330–370 nm. $K_2Pt(CN)_4$ emits only in the blue region with a maximum at 465 nm, while crystals of $TlNO_3$ and $TlCH_3CO_2$ are very weakly, if at all, emissive under the excitation conditions.

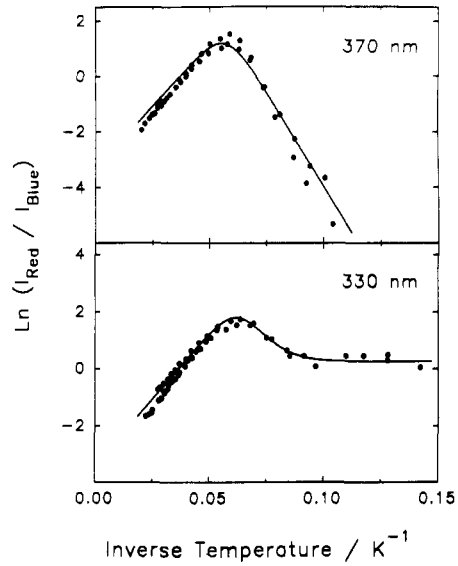

Figure 4. Arrhenius plot of the peak intensity ratio I_{red}/I_{blue} of $Tl_2Pt(CN)_4$ for 370- (top) and 330-nm (bottom) excitation. The solid lines are calculated from the kinetic model discussed in the text.

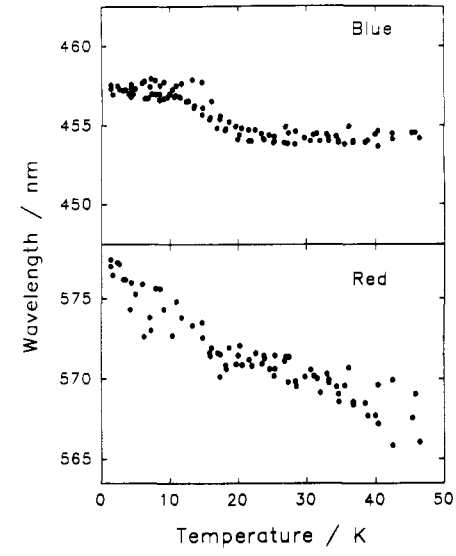

Figure 5. Peak wavelength of the blue (top) and red (bottom) bands of $Tl_2Pt(CN)_4$ as a function of temperature, showing the 2.9-nm shift of the blue band between 10 and 20 K.

blue and red bands of the colorless crystals plus additional bands. At 300 K, the emission spectrum of the colored powder shows a single broad band peaking at ≈570 nm with a photoexcitation maximum at 415 nm. Its mull absorption spectrum at 300 K shows a maximum at ≈370 nm with a shoulder at ≈415 nm. Below 77 K, additional emission bands appear. The major bands at 1.4 K occur at 460, 510, and 590 (±3) nm with corresponding photoexcitation maxima at 375, 390, and 335 (±3) nm, respectively. For 370-nm excitation, the 460-nm band has the greatest peak intensity by a factor of roughly 3. For 330-nm excitation, the 590-nm band has a slightly greater peak intensity than the 460-nm band, while the 510-nm band is relatively weak and unresolved. Hence, the intensity changes in the blue and red bands in the colored powder for 370- and 330-nm excitation parallel the changes seen in the colorless crystals. This supports the idea that the blue and red bands are intrinsic to $Tl_2Pt(CN)_4$ at low temperatures. The spectra of the colored powder were not examined in further detail.

Luminescence Lifetimes. The decay kinetics of the blue and red bands of the colorless form, following pulsed excitation at 337 nm, were investigated as a function of temperature between 1.4 and 30 K and as a function of applied magnetic field at 1.4

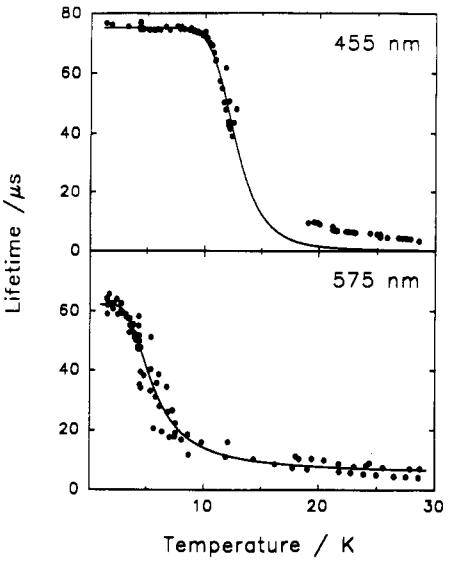

Figure 6. Lifetime of the blue (top) and red (bottom) bands of $Tl_2Pt(CN)_4$ between 1.4 and 30 K. The solid lines are calculated lifetimes as discussed in the text.

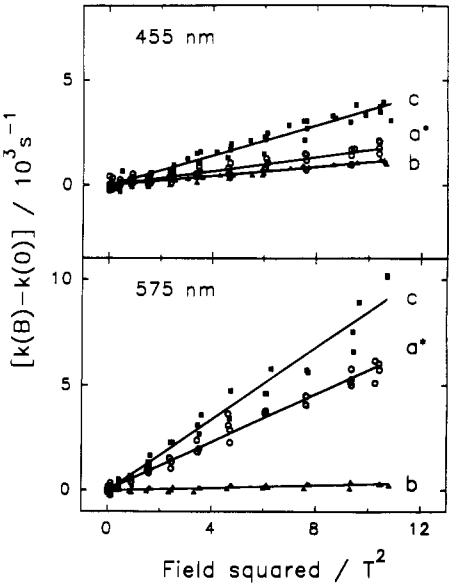

Figure 7. Change in the depopulation rates of the blue (top) and red (bottom) bands of $Tl_2Pt(CN)_4$ at 1.4 K with applied magnetic field along three orthogonal crystal axes, showing the linear dependence on the square of the applied field strength. The solid lines are based on the slopes given in Table II.

K. Both temperature variation and applied magnetic fields caused strong perturbations of the decays. The decays showed poor fits to a single-exponential form (over a three-decade change in intensity beginning ≈500 ns after the excitation pulse), independent of the excitation intensity. This was most notable for the blue band in the temperature range where its decay was most strongly dependent on temperature. Much better fits resulted with the assumption of a bi- or triexponential form. Hence, all decays over the entire temperature range studied were analyzed as a sum of two or three exponentials, even though the relative amplitudes of the minor components were often quite small. We report only the lifetime of the major component for those temperatures where its relative amplitude at zero time was ≥70%. Henceforth, we refer to this major component simply as the lifetime. The lifetimes at select temperatures are included in Table I. These were established to be independent of polarization in *bc* at 1.4 K.

The dependences of the lifetimes on temperature below 30 K are shown in Figure 6. These show an abrupt decrease with increasing temperature at about 5 and 12 K for the red and blue bands, respectively. Hence, an additional channel for depopulation becomes thermally accessible at the corresponding temperature for the excited state of each band. Since the emission intensity of the red band remains constant over the temperature range of its lifetime shortening, its additional channel appears radiative. However, since the emission intensity of the blue band decreases concurrently with its abrupt lifetime shortening, its additional channel appears nonradiative.

The temperature dependence of the lifetime between 1.4 and 30 K could be reasonably fit to a Boltzmann equilibrated model for the red band, but not for the blue band. The lifetime of a group of levels in Boltzmann equilibrium is given by[11]

$$\tau = \frac{g_a + g_b \exp(-E_{ba}/kT) + \dots}{g_a k_a + g_b k_b \exp(-E_{ba}/kT) + \dots} \qquad (1)$$

where the levels have degeneracies g_i, total depopulation rates k_i, and energies E_i, with $E_{ij} = E_i - E_j$. The solid line in Figure 6 (bottom) shows a fit of the experimental data for the red band to eq 1 for a pair of levels using a weighted least-squares algorithm. The parameters deduced using weights derived from a constant percent error in the experimental lifetimes and assuming degeneracies of $g_a = 1$ and $g_b = 2$ are $1/k_a = 62.5$ μs, $1/k_b = 2.95$ μs, and $E_{ba} = 14.5$ cm^{-1}. As evident from Figure 6 (bottom), eq 1 with these parameters yields good agreement with the experimental data for the red band.

The lifetime data for the blue band could not be explained using eq 1. The lifetime changes too steeply with temperature to be consistent with the observed lifetimes at <8 and >20 K. Either a much shorter lifetime at >20 K or a much more gradual change with temperature is required for a Boltzmann equilibrated pair of levels with $g_i \leq 2$. We conclude that the temperature variation of the lifetime for the blue band cannot be explained adequately by a simple Boltzmann equilibrated model. An earlier report[7a] of lifetime data for the blue band between 1.7 and 40 K appeared to fit a Boltzmann equilibrated model. However, this conclusion was based on limited data, particularly in the temperature range between 10 and 20 K. Close examination of the earlier data, which was also nonexponential in the range 10–20 K, indicates no significant discrepancies between the two sets.[7b] The present conclusion also gains support from the observed decrease with increasing temperature in the steady-state intensity of the blue band over the range where its lifetime decreases. Hence, the lifetime and intensity decreases appear to be related and to be due to a thermally activated radiationless depopulation of the excited state of the blue band.

A Zeeman field causes a shortening of the lifetime at 1.4 K for both the blue and red bands. These changes depend on both the orientation and magnitude of the field. There are, however, no detectable changes in either the intensities or peak wavelengths of the bands under steady-state conditions. Figure 7 shows plots of the change in the rates (inverse lifetimes) versus the square of the applied magnetic field strength for three orthogonal orientations of the field relative to the crystal axes for both bands. The plots are linear over the field strengths investigated.[12] The slopes are summarized in Table II and yield the solid lines shown in Figure 7.

Magnetic field effects on decays generally result from the mixing of other states into the emissive state by the Zeeman

(11) Azumi, T.; O'Donnell, C. M.; McGlynn, S. P. *J. Chem. Phys.* **1966**, *45*, 2735. Harrigan, R. W.; Crosby, G. A. *J. Chem. Phys.* **1973**, *59*, 3468. Hager, G. D.; Crosby, G. A. *J. Am. Chem. Soc.* **1975**, *97*, 7031.

(12) The rates from single-exponential fits are also linearly dependent on the square of the applied field, and show, as expected, less scatter and slightly different parameters. The rates of the minor components from the biexponential fits that were employed for the data in Figure 7 do not depend linearly on the square of the field.

Table II. Dependence of the Depopulation Rates of the 455- and 575-nm Emission Bands of $Tl_2Pt(CN)_4$ on Magnetic Field at 1.4 K

	slope/10^5 s^{-1} T^{-2}	
axis	455 nm	575 nm
a^*	1.7	5.7
b	1.1	0.31
c	3.6	8.5

interaction.[13] If the energy gaps from these emissive states to other states are large with respect to the Zeeman energy, the mixing can be discussed using perturbation theory. The coefficients of the mixed-in states will then depend linearly on the field strength, leading to a quadratic dependence of the squared transition moment to the ground state (radiative depopulation rate) on the magnitude of the applied magnetic field. In general, the maximum effect will occur for a particular orientation of the magnetic field and depend on both the operative energy denominators and the transition moments of the mixed-in states. The nonradiative rate to the ground state can also be enhanced by Zeeman mixing. This can lead to either a linear or a quadratic dependence on the field strength.[13] The increase in the total depopulation rate with the square of the field strength for the red band implies that the important mixed-in states have larger transition moments for decay to the ground state than the unperturbed emitting state. The interpretation for the blue band is less clear, since a nearby state may exist that leads to rapid radiationless depopulation of the emissive state.

For both bands, the mixing is a maximum for the magnetic field oriented perpendicular to the Tl–Pt (z) molecular axis. The direction cosines of the z axis, as calculated from the structure determination,[6] are 0.447, –0.815, and –0.368 for the a^*, b, and c crystal axes, respectively, where a^* is orthogonal to b and c. The experimental slopes, as seen from Figure 7 and Table II, are largest for $\mathbf{B} \parallel \mathbf{c}$ and smallest for $\mathbf{B} \parallel \mathbf{b}$, with the slopes for the red band showing the greater anisotropy. Hence, the slopes order oppositely to the magnitudes of the direction cosines for the z axis, pointing to a maximum effect for the magnetic field oriented perpendicular to the z axis.

The decay kinetics for the impure, yellow form of $Tl_2Pt(CN)_4$ were examined only cursorily. However, insofar as investigated, the lifetimes for the blue and red bands are similar to those of the colorless crystals. The lifetime for the blue band is essentially identical to that in the colorless crystals over the temperature range examined (1.4–15 K). The decay of the red band is more nonexponential in the colored powder with a major component of ≈50 μs at 1.4 K. We assume that the greater degree of nonexponentiality for the red band is associated with the presence of additional, overlapping emission bands in the colored powder.

Discussion

The temperature dependence of the steady-state intensities and the sensitivity of the decays to temperature and applied magnetic field in the noncolumnar compound $Tl_2Pt(CN)_4$ parallel to some degree the behavior seen in the columnar compounds of $Pt(CN)_4^{2-}$.[1] However, significant differences exist. In the columnar compounds at low temperature, the higher energy of the two observed emission bands is very short-lived, and it overlaps the absorption. Accordingly, the higher energy emission is generally assigned as fluorescence from a free exciton state associated with the columnar chains of $Pt(CN)_4^{2-}$ moieties. The lower energy emission has a much longer lifetime that is strongly perturbed by temperature variation and magnetic fields. It is assigned to nominal phosphorescence from a self-trapped exciton. The large spin–orbit interactions engendered by the Pt center lead to a correspondingly large "zero-field splitting" among the components of the emitting triplet state (20–40 cm^{-1}).[1] These

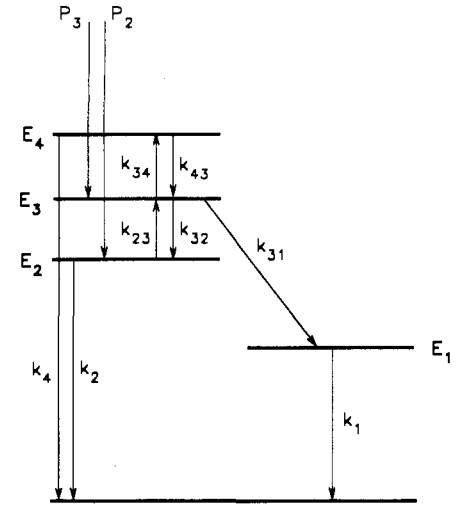

Figure 8. Schematic energy level diagram showing the nonzero rates considered in the kinetic model discussed in the text.

nearby components then account in large part for the temperature and magnetic field effects on the properties of the lower energy emission band.

In $Tl_2Pt(CN)_4$ at 1.4 K, the blue emission band is relatively long-lived, and it shows no overlap with the onset of the absorption (extrapolated origins differ by ≥2000 cm^{-1}). Hence, within the spin-label limitations imposed by the expected strong spin–orbit interactions, a forbidden singlet or nominal triplet assignment is suggested for the excited state of the blue band. Although either possibility can allow the perturbation of its lifetime by a magnetic field, only a nominal triplet assignment seems consistent with the low-temperature lifetime of 77 μs. Even a symmetry-forbidden singlet state is expected to have a shorter (radiative) lifetime, due to allowedness gained from crystal field and vibronic interactions. However, a similar conclusion follows also for the red band. Indeed, its decay is more strongly perturbed by a magnetic field, and the temperature dependence of its decay can be described in terms of a Boltzmann equilibrium among close-lying spin–orbit levels. Hence, it appears that two nominal triplet states are emissive in $Tl_2Pt(CN)_4$ at 1.4 K, leading to the blue and red bands. We postpone a consideration of the identification of these states until after a kinetic model is presented. The chosen model is prompted by studies of the temperature dependence of the relative emission intensities from self-trapped and delocalized exciton states in columnar compounds of $Pt(CN)_4^{2-}$.[1,14]

Kinetic Model. We consider a model with four excited levels as shown in Figure 8. The levels have energies E_i, populations n_i, total (radiative plus nonradiative) depopulating rates to the ground state k_i, radiative emission rates to the ground state k_i^r, and populating rates by the exciting light P_i. The radiationless transfer of population from n_i to n_j for $E_j > E_i$ is assumed governed by the thermally activated rate $k_{ij} = k_{ij}^0 \exp(-E_{ji}/kT)$ where $E_{ji} = E_j - E_i$. The red band arises from n_1, which we take as the total population associated with a Boltzmann equilibrium over levels n_{1a} and n_{1b}, as discussed earlier following eq 1. The blue band arises from some combination of n_2, n_3, and n_4.

The model is simplified by choosing the minimum number of rates as nonzero, while reasonably accounting for the experimental observations. Since the energy difference between the blue and red bands is much greater than kT over the temperature range studied, we set all $k_{1j} = 0$ ($j = 2, 3, 4$). We further assume that n_1 is populated only by relaxation from n_3 (k_{31}). Significant population of n_1 directly from n_2 cannot occur since $I_{red}/I_{blue} \approx 0$ for 370-nm excitation at <10 K, so that $k_{21} = 0$. Similarly, n_1 cannot be populated significantly from direct excitation (P_1

(13) Gliemann, G. *Comments Inorg. Chem.* **1986**, *5*, 263.

(14) Gliemann, G.; Holzapfel, W.; Yersin, H. *J. Phys., Colloque* **1985**, *C7*, 129.

= 0) or directly from n_4 (k_{41} = 0) since $I_{red}/I_{blue} \approx 0$ for all excitation energies at >40 K. Since I_{blue} is minimum when I_{red} is maximum, we neglect any radiative depopulation of n_3 to the ground state (k_3^r = 0) and assume that I_{blue} arises from just n_2 and n_4. Nonradiative depopulation of n_3 (k_3 = 0) and direct population of n_4 (P_4 = 0) are also neglected for simplicity, although the results are not materially affected by their inclusion. The various rates that are taken as nonzero are shown in Figure 8.

At steady state, the populations are given by

$$n_1^0 = (P_2K_4k_{23}k_{31} + P_3K_2K_4k_{31})/k_1D \quad (2a)$$

$$n_2^0 = (P_2(K_3K_4 - k_{34}k_{43}) + P_3K_4k_{32})/D \quad (2b)$$

$$n_3^0 = (P_2K_4k_{23} + P_3K_2K_4)/D \quad (2c)$$

$$n_4^0 = (P_2k_{23}k_{34} + P_3K_2k_{34})/D \quad (2d)$$

where

$$D = K_2K_3K_4 - K_2k_{34}k_{43} - K_4k_{23}k_{32} \quad (3)$$

and $K_2 = k_2 + k_{23}$, $K_3 = k_{31} + k_{32} + k_{34}$, and $K_4 = k_4 + k_{43}$. The resulting emission intensities are given by $I_i = Ck_i^r n_i^0$, where C is an experimental constant, and become

$$I_1 = CP_2Q_1[Pa + (1 + P)b \exp(-E_{32}/kT)]/D' \quad (4a)$$

$$I_2 = CP_2Q_2[1 + P(1 - a) + c \exp(-E_{43}/kT)]/D' \quad (4b)$$

$$I_3 = 0 \quad (4c)$$

$$I_4 = CP_2Q_4[Pc \exp(-E_{43}/kT) + (1 + P)d \exp(-E_{42}/kT)]/D' \quad (4d)$$

where

$$D' = 1 + b \exp(-E_{32}/kT) + c \exp(-E_{43}/kT) + d \exp(-E_{42}/kT) \quad (5)$$

The remaining definitions are $Q_i = k_i^r/k_i$, $P = P_3/P_2$, $a = k_{31}/(k_{31} + k_{32})$, $b = ak_{23}^0/k_2$, $c = k_4k_{34}^0/K_4(k_{31} + k_{32})$, and $d = bc/a$.

At sufficiently low temperature that $kT \ll E_{32}$ or E_{43}, the levels are decoupled. The nonzero emission intensities are then simply

$$I_1 = CP_2Q_1Pa \quad (6a)$$

$$I_2 = CP_2Q_2[1 + P(1 - a)] \quad (6b)$$

We assume that, following excitation at 370 and 330 nm, fast relaxation occurs to n_2 and n_3, respectively. Thus, we associate 370- and 330-nm excitation with P_2 and P_3, respectively. Hence, only n_2 emits at low temperature with an intensity $I_2 = CQ_2P_2$ for 370-nm excitation. However, both n_1 and n_2 emit even at low temperature for 330-nm excitation with their relative intensities dependent on the branching ratio from n_3, a, and the relative radiative quantum yields, Q_i.

As the temperature increases, at first n_2 decreases and n_1 increases for excitation by P_2 or P_3, due to the thermally activated removal of population from n_2 into n_3 and the subsequent increase in the population of n_1 by relaxation from n_3. Hence, I_{blue} decreases while I_{red} increases with I_{red}/I_{blue} showing an Arrhenius activation energy of E_{32}. However, further temperature increase causes population of n_4 and the onset of an additional radiative channel associated with the blue band. A blue shift and an intensity increase for the blue band, with a corresponding intensity decrease for the red band, result. I_{red}/I_{blue} now decreases with a limiting Arrhenius activation energy of E_{43}.

Table III. Model Parameters

$k_{1a}/10^4$ s^{-1}	1.6	g_{1b}	2
g_{1a}	1	E_{1ba}/cm^{-1}	14.5
$k_{1b}/10^4$ s^{-1}	0.34		
a	0.75	Q_4/Q_2	0.80
$b/10^4$	3.1	P_3/P_2	90
c	13	E_{32}/cm^{-1}	94.
Q_1/Q_2	0.45	E_{43}/cm^{-1}	65.

Values for the parameters of the model were deduced by trial to approximately reproduce the temperature dependence of the experimental intensities, given by $I_{blue} = I_2 + I_4$ and $I_{red} = I_1$, and the ratio I_{red}/I_{blue}. The parameters found are summarized in Table III. We assumed that the Q_i were temperature independent, which for Q_1 requires that $k_{1n}^r/k_{1n} = 1$. However, the fact that Q_1/Q_2 is not unity is insignificant, since the experimental data refer to uncorrected peak rather than corrected integrated intensities. Accounting for the greater width of the red band (roughly a factor of 2) would increase Q_1 accordingly. The calculated results from the model using the parameters in Table III are included in Figures 3 and 4 as solid lines. These show good qualitative agreement with the experimental intensity data for both 370- and 330-nm excitation. Further, the observed shift in the peak wavelength of the blue band (140 cm^{-1}) is in rough agreement with the value of E_{42} (160 cm^{-1}) derived from the model.

For $kT \ll E_{ij}$, each n_i decays as a single exponential with rate k_i, so that the major rates observed for the red and blue bands at 1.4 K reduce to k_1 and k_2, respectively. As the temperature increases, the major decay component for the red band retains the rate k_1 (Boltzmann averaged) since no additional channel for depopulation of n_1 becomes accessible. The decay kinetics for the blue band are more complicated, becoming in general a sum of exponential components due to the coupling among the levels. However, its major decay component, k_{blue}, will increase with increasing temperature. As a first approximation, valid for temperatures where k_{blue} begins to increase and the contribution of n_4 to the intensity is negligible, $k_{blue} \approx k_2 + k_{23}$. The value of k_{23}^0/k_2 obtains from the model as b/a. Hence, $k_{blue} \approx k_2 + k_2(b/a) \exp(-E_{32}/kT)$. The values of $1/k_{blue}$, calculated using b/a and E_{32} from Table III and $1/k_2$ from Table I, are included in Figure 6 (top) as the solid line.

The agreement with the experimental lifetime data for the blue band is quite good at ≤15 K. However, the observed lifetimes appear to deviate from the predictions of the model at higher temperatures. We assume that this is due to the simplicity of the model. A more detailed analysis, however, is not warranted by the available data and the uncertainties associated with the deconvolution of the observed nonexponential decays. The identifications of the parameters implied by the model should be judged accordingly.

Tentative Assignments. The model allows the blue and red bands to be associated with the same or different centers. If the same center is involved, the results indicate unusual relaxation among the excited states with multiple states having the same nominal triplet multiplicity, but significantly different energies (≈4000 cm^{-1}), emissive. The simpler explanation is that the two bands are not associated with the same center. The similarities in the spectra of the colorless crystals and the colored powder then suggest that at least two emissive centers are intrinsic to $Tl_2Pt(CN)_4$, insofar as the impurities causing the coloration of the powder form do not appear to impact significantly upon the excitation energy dependence of the blue and red bands at 1.4 K, the gross temperature dependence of their intensities at ≤77 K, or their lifetimes at 1.4 K. The different excitation spectra are also more readily accommodated with two emissive centers.

The red band (n_1) is accordingly tentatively assigned to the triplet state of a strongly perturbed (deeply trapped) $Tl_2Pt(CN)_4$

moiety. This is possibly associated with a ubiquitous crystal defect or impurity. Two of its spin–orbit components are split by 15 cm^{-1}, with the longer lived and less allowed component lower in energy. The relative populations of these components remain in Boltzmann equilibrium over the temperature range studied. The blue band is similarly assigned to the triplet state(s) of an unperturbed or weakly perturbed $Tl_2Pt(CN)_4$ moiety. The lowest energy emissive level (n_2) of the blue band corresponds to the lowest energy spin–orbit component of such a triplet state.

These assignments seem quite reasonable from a comparison of the energies of the observed states with the expected energies in columnar $Pt(CN)_4^{2-}$ systems for a given Pt–Pt separation distance, R. The latter energies can be obtained from known empirical relations.[1] For the monomeric anion ($R = \infty$), the higher energy, z-polarized (singlet) absorption and the lower energy, xy-polarized (triplet) emission bands are predicted to occur at 220 and 272 nm, respectively. For R = 3.14 Å, corresponding to the Tl–Pt distance in $Tl_2Pt(CN)_4$, the bands are predicted at 509 and 608 nm. These extrapolations yield apparent splittings between the singlet and triplet excited states of 8700 and 3200 cm^{-1}, respectively. In $Tl_2Pt(CN)_4$, the singlet state is observed in photoexcitation and absorption at 375 nm and the triplet state in emission at 457 nm, yielding a splitting of 4800 cm^{-1}. Hence, the results for the blue band of $Tl_2Pt(CN)_4$ are intermediate to the above two limits. This result can be anticipated for comparable interactions between an infinite and a finite (Tl-Pt-Tl "trimer") chain. The width of the "band" will be smaller in the finite system, leading to a smaller red shift of the states. For example, trimers of $Pt(CN)_4^{2-}$ in aqueous solution absorb at ≈300 nm and emit at ≈350 nm,[2] showing an energy splitting of ≈4750 cm^{-1}. The greater red shifts of the bands in $Tl_2Pt(CN)_4$ relative to the trimer suggest that the Tl–Pt interactions are greater than the Pt–Pt interactions, in agreement with the noncolumnar crystal structure of $Tl_2Pt(CN)_4$.

The red emission band at 577 nm and its photoexcitation maximum at 335 nm yield a much too large splitting (12.5×10^3 cm^{-1}) to associate with nominal triplet and singlet excited states, respectively, on the basis of a similar extrapolation of the energies in columnar $Pt(CN)_4^{2-}$ systems. This prompts our assignment of the red band to a strongly perturbed $Tl_2Pt(CN)_4$ moiety. Alternatively, the 335-nm band could represent a higher excited state of bulk $Tl_2Pt(CN)_4$ from which relaxation to the excited state of the red band is facile. The singlet state of the deep trap would then be unobserved.

Identifications of the levels n_3 and n_4 are less readily conjectured. Possible assignments must account for the relatively greater radiative activity of n_4 and for the absence of population of n_1 by direct relaxation from n_2. The greater activity of n_4 can occur if it is dipole allowed in transition with the ground state while n_3 is dipole forbidden. The selective population of n_1 only by relaxation from n_3 and/or n_4 is more problematic, particularly if n_2, n_3, and n_4 are associated with components (spin–orbit or vibronic) of a single excited state. The difficulties are minimized if n_2 corresponds to a $Tl_2Pt(CN)_4$ moiety in a shallow trap, while n_3 and n_4 are associated with triplet exciton bands of bulk $Tl_2Pt(CN)_4$. Population of n_3 could then lead to a branching between the shallow (n_2) and deep (n_1) traps by energy transfer associated with mobile excitons. The level n_4 would correspond to the lowest energy, strongly allowed level in the triplet exciton bands. The energy gap E_{43} would reflect either an intramolecular spin–orbit splitting or an intermolecular (Davydov) interaction, depending on the relative magnitudes of the two terms.

On the basis of the similarity to the spin–orbit splittings in the columnar systems and the expectation of weak intermolecular interactions between $Tl_2Pt(CN)_4$ moieties in the crystal, we assign E_{43} as the spin–orbit splitting in the lowest triplet state of $Tl_2Pt(CN)_4$. The lower energy component (n_3) is forbidden in transition with the ground state while the higher energy component (n_4) is allowed. Both components presumably form narrow bands through which energy transfer to the traps n_2 and n_1 can occur. However, at low temperatures the dynamics favor the population of n_1 predominantly through the lower energy band associated with n_3.

The suggested identifications of the levels of the model lead to similar properties for the excited triplet states of the blue and red bands. Both states involve a pair of spin–orbit components with the less allowed component lower in energy, and both have comparable magnitudes for the splitting between the components (65 and 15 cm^{-1}). Other components of the triplet state associated with n_2 are unobserved within the conjectured assignments. However, since the properties of a shallow trap are not expected to grossly differ from those of the unperturbed molecule, we expect that the spin–orbit splitting in the shallow trap is also near 65 cm^{-1} with the more allowed component above n_2. The other component is, thus, close to the bands associated with n_3 and n_4, and it is not unreasonable that it would not act as a strongly emissive level at temperatures where it (and n_3 and n_4) would be populated. The increased degree of nonexponentiality in the decay of the blue band between ≈12 and 20 K may reflect contributions from other components associated with n_2.

Calculations agree that the lowest energy excitation of $Tl_2Pt(CN)_4$ in the D_{4h} point group is π^* (a_{2u}) ← d, but the symmetry of the d orbital involved varies.[5,8] The $d_{x^2-y^2}$ (b_{1g}) orbital, from simple crystal field ideas and electronic structure calculations,[4,5,8] can be excluded from consideration because of the strong tetragonal distortion of $Tl_2Pt(CN)_4$. The possible assignments for the lowest triplet state are then ^3E_u from $d_{xz,yz}$ (e_g), $^3A_{2u}$ from d_{z^2} (a_{1g}), and $^3B_{1u}$ from d_{xy} (b_{2g}). Each of these assignments has spin–orbit components that are electric dipole allowed in transition with the $^1A_{1g}$ ground state. The available experimental results do not allow an unambiguous differentiation among these possibilities, although the ^3E_u assignment appears least favored. As discussed for the ^3E_u manifold in porphyrins by Gouterman et al.[15] and van der Waals et al.,[16] the splittings among the components of ^3E_u are governed by the spin–orbit, spin–spin, Jahn–Teller, and crystal field interactions. If only the spin–orbit interactions are considered, three doubly degenerate and equally spaced levels result ($A_{1u} + A_{2u}$, $J_z = 0$; E_u, $J_z = \pm 1$; $B_{1u} + B_{2u}$, $J_z = \pm 2$). Since only A_{2u} and E_u are allowed in electric-dipole transition with the A_{1g} ground state, either the two lowest or two highest energy levels are emissive ($J_z = 0, \pm 1$). If the Jahn–Teller and crystal field interactions are dominant, the spatial degeneracy of ^3E_u is removed with a particular distortion stabilized by the crystal field. The lowest state now acts like a "normal" triplet state with its three components split by the relatively smaller spin–orbit and spin–spin interactions. An asymmetric splitting pattern would result, and allowed transitions to the ground state from two components are expected within the lower symmetry point group of the distortion. Hence, if the observed triplet states were derived from a ^3E_u assignment, two components should be active. The experimental results, however, favor triplet states with a pair of spin–orbit components having significantly different activities for both the blue and red bands.

Either the $^3A_{2u}$ or $^3B_{1u}$ assignment can yield two "resolved" components with only one (E_u) dipole allowed to the ground state when the spin–orbit interactions are large relative to the crystal field and spin–spin terms. Either possibility can also provide rough qualitative agreement with the experimental Zeeman results. Consider, for example, the $^3A_{2u}$ assignment with spin–orbit components E_u and A_{1u}, which we order with the allowed E_u component higher in energy. The lifetime of the forbidden A_{1u} component will be derived from crystal field and vibronic

(15) Gouterman, M.; Yamanashi, B. S.; Kwiram, A. L. *J. Chem. Phys.* **1972**, *56*, 4073.
(16) Kooter, J. A.; Canters, G. W.; van der Waals, J. H. *Mol. Phys.* **1977**, *33*, 1545. van Dijk, N.; Noort, M.; Voelker, S.; Canters, G. W.; van der Waals, J. H. *Chem. Phys. Lett.* **1980**, *71*, 415.

interactions and, thus, will be relatively long. Zeeman mixing will occur for **B** ∥ **z** between A_{1u} and A_{2u} states and for **B** ∥ **xy** between $E_u^{(a)}$ and A_{2u} states and between $E_u^{(b)}$ and A_{1u} states. Hence, the forbidden A_{1u} level is directly mixed with the nearby allowed E_u level only for **B** ∥ **xy**. As noted earlier, this is consistent, assuming bulk direction cosines, with the observed anisotropies in the magnitude of the lifetime shortening caused by a Zeeman field in the decay of both the blue and red bands. The larger Zeeman effect for the red band than for the blue band for **B** ∥ **a*** and **c** may result simply from the smaller spin–orbit splitting in the deep trap (15 cm^{-1}) than in the shallow trap (≥65 cm^{-1}).

The I_b/I_c polarization ratio at 1.4 K indicates a mixed polarization for both bands. This is again not inconsistent with their identifications as traps with the emissions at 1.4 K arising from nominally forbidden spin–orbit components which derive intensity from crystal field and vibronic interactions. In terms of the bulk direction cosines, the observed ratio (0.6) implies predominantly *xy* polarization, so that the emissions from the forbidden spin–orbit components derive largely from E_u states in D_{4h} symmetry. The increase in the ratio for the blue band at higher temperature (0.8 at 300 K) suggests an increased contribution of A_{2u} states to the intensity at higher temperatures.

Summary

The results for the noncolumnar compound $Tl_2Pt(CN)_4$ show both similarities to and differences from the columnar compounds of $Pt(CN)_4^{2-}$. Both systems show two emission bands with their relative intensities similarly dependent on temperature. The lower energy of the two bands also has a nominal triplet parentage in the two systems. However, the higher energy band also derives from a nominal triplet state in $Tl_2Pt(CN)_4$, whereas in the columnar systems the higher energy band is associated with very short-lived fluorescence from a singlet exciton state. The spin–orbit interactions in $Tl_2Pt(CN)_4$ are expected to be large and cause considerable mixing among the excited states, so that the spin-labels will loose validity. However, the blue band of $Tl_2Pt(CN)_4$ cannot be assigned to the lowest energy, singlet exciton state, due to its long lifetime and considerable energy gap from the onset of absorption. The observed differences relate in part to the different crystal structures. The columnar systems are quasi-one-dimensional, whereas $Tl_2Pt(CN)_4$ is not. This is particularly apparent in the data from the polarizations of the emissions and the Zeeman perturbations. In addition, the Tl–Pt interactions are different in detail from the Pt–Pt interactions. This is apparent in the comparison of the observed energies with the extrapolated energies, based on the columnar systems, of the lower excited states for the metal–metal distance in $Tl_2Pt(CN)_4$.

A dependence of the emission spectrum on excitation energy has been observed in the columnar system $BaPt(CN)_4 \cdot 4H_2O$, wherein it has been attributed to different processes governing the relaxation from different initially excited states.[1] Similar atypical relaxation occurs in $Tl_2Pt(CN)_4$. Excitation at 370 nm leads to population at low temperatures of an excited nominal triplet state of a shallow trap. Excitation at 330 nm, however, involves relaxation paths which populate the lowest triplet exciton bands of bulk $Tl_2Pt(CN)_4$, from which nominal triplet states of both a shallow and a deep trap are populated.

Acknowledgment. We thank Professor J. K. Nagle for providing us with his kinetic data in advance of publication, along with some of his sample of $Tl_2Pt(CN)_4$, and for comments on the paper. We also thank the UCD Committee on Research for providing support under its Collaborative Research Project (A.L.B. and D.S.T.).